ACADEMIC PRESS

Available online at www.sciencedirect.com
SCIENCE DIRECT

Journal of Catalysis 215 (2003) 188–198

JOURNAL OF CATALYSIS

www.elsevier.com/locate/jcat

The interaction of hydrogen with alumina-supported copper catalysts: a temperature-programmed adsorption/temperature-programmed desorption/isotopic exchange reaction study

H. Wilmer, T. Genger,[1] and O. Hinrichsen *

Laboratory of Industrial Chemistry, Ruhr-University Bochum, D-44780 Bochum, Germany

Received 20 June 2002; revised 22 October 2002; accepted 14 November 2002

Abstract

The interaction of hydrogen with a series of copper catalysts (Cu/Al_2O_3, Cu/ZnO, and $Cu/ZnO/Al_2O_3$) was studied by combining temperature-programmed (TP) techniques and the isotopic exchange reaction of H_2 and D_2 with microkinetic modeling. Various TP experiments (TP desorption, TP adsorption) were carried out, resulting in a set of kinetic parameters for a quantitative description. Only small differences in the kinetics of the ZnO-containing Cu catalysts and Cu/Al_2O_3 were observed, suggesting that the interaction of H_2 with the Cu surface is therefore only slightly influenced by the presence of zinc oxide, and alumina seems to act only as a structural promoter. Significant changes in the results were found when the treatment prior to the actual experiments was altered. From these observations and further supporting experiments it was deduced that a change in the morphology of the metallic Cu particles and surface alloying occur under more severe reducing conditions. These dynamical changes seem to be highly relevant for methanol synthesis.

Keywords: Hydrogen; Cu catalysts; Microkinetics; Adsorption; Desorption; H_2 TPD; H_2 TPA; IER; Methanol synthesis

1. Introduction

Copper has received considerable attention as a model system to study the interaction of hydrogen with metal surfaces in detail [1,2]. However, this is a subject not only of great complexity, but also of enduring controversy. Beginning with the pioneering work of Balooch et al. [3], extensive research on different single crystal surfaces has been carried out by numerous research groups in recent decades [4–15] to obtain a deeper understanding of the kinetics of adsorption and desorption. It is now generally accepted that the adsorption process of hydrogen on Cu is activated [4,5,8–12,14]. The dynamics and energetics of the adsorption of H_2 on Cu(110) were probed by Hayden et al. [8,9,11] and by Campbell and Campbell [12] in detail. Their results provided experimental evidence that the chemisorption of hydrogen occurs by a direct dissociative mechanism which was found to be activated with an Arrhenius activation energy of about 57 $kJ\,mol^{-1}$. Similar values were found by Rasmussen et al. [14] from sticking probability measurements of H_2 and D_2 on Cu(100). The temperature-programmed desorption (TPD) of hydrogen from Cu single crystal surface measurements was studied in detail by Anger et al. [10]. While the desorption follows ideal second order on Cu(111), hydrogen causes restructuring of the Cu surface on Cu(100) and Cu(110). These observations were confirmed by several research groups [7,11,16,17].

Metallic Cu was found to be the active component in Cu-based catalysts for methanol synthesis. Nowadays, $Cu/ZnO/Al_2O_3$ catalysts are employed commercially in the low-pressure low-temperature methanol synthesis process and in the low-temperature water–gas shift reaction [18,19]. Recently, the kinetics of desorption of hydrogen from ternary Cu catalysts were obtained independently by different research groups [20–22] in detail bridging the *pressure* and *material* gaps between surface science and catalysis under relevant reaction conditions. Furthermore, Tabatabaei et al. [23] applied hydrogen-reactive frontal chromatography to study the kinetics of adsorption on Cu/Al_2O_3. They de-

* Corresponding author.
E-mail address: olaf@techem.ruhr-uni-bochum.de (O. Hinrichsen).
[1] Present address: BASF AG, GCE/B, D-67056 Ludwigshafen, Germany.

0021-9517/03/$ – see front matter
doi:10.1016/S0021-9517(03)00003-4

rived an activation energy of 42 kJ mol^{-1}, which is somewhat lower than that derived in single crystal studies.

Despite the efforts to contribute to a better understanding of the H_2 interaction with copper/zinc/alumina catalysts of industrial interest, there exist, to the best of our knowledge, no explicit presentation so far which includes and compares experiments obtained with the basic coprecipitated samples, namely ZnO/Al_2O_3, Cu/Al_2O_3, Cu/ZnO, and $Cu/ZnO/Al_2O_3$. Since complications due to the interaction of H_2 with zinc oxide are discussed in the literature [23–29], we present a detailed kinetic study to gain a deeper understanding of metal support interactions in copper/zinc/alumina catalysts. Since the adsorption of hydrogen on Cu is an activated process, it is possible to derive the kinetic parameters from various transient experiments conducted with a systematic series of copper/zinc/alumina catalysts in a microreactor flow system operating under industrially relevant reaction conditions. Experiments comprised temperature-programmed techniques (H_2 TPD and H_2 temperature-programmed adsorption (TPA)) and the isotopic exchange reaction (IER) of H_2 and D_2.

Finally, we performed a microkinetic analysis based on our experiments. We have chosen a simple Langmuirian approach with coverage-independent Arrhenius parameters for the modeling to compare the microkinetics of hydrogen interaction with Cu-based catalysts. We applied the heating rate variation as a method to extract kinetic parameters to support our experimental results with physically reasonable Arrhenius parameters. There are a variety of other methods, which have been shown to be highly suitable in single crystal studies [30,31], but their application would result in coverage-dependent preexponential factors and activation energies. In general, the method of heating rate variation leads to mean values of these kinetic parameters because the evaluation spans the full range of coverage, neglecting any adsorbate–adsorbate interaction. In an earlier publication [32], we presented a detailed analysis of the desorption kinetics of hydrogen from a ternary Cu catalyst and compared the results with the single crystal literature. On the other hand we showed for the same example that the method of heating rate variation is an effective tool for extracting desorption parameters [21].

2. Experimental

The Cu/Zn/Al hydroxycarbonate precursors were prepared by conventional coprecipitation from an aqueous solution of metal nitrates using an aqueous solution of Na_2CO_3 as precipitating agent. Good reproducibility and comparability were attained by carefully controlling the preparation conditions (purity of the chemicals, concentrations, temperature, pH value, aging time, and washing treatment). The precipitates were washed to remove the Na, filtered, dried in air at 393 K, and calcined in air at 603 K. A detailed description of the preparation method and characterization results are given in [33]. To examine the influence of the different components on the interaction with hydrogen, the following samples were studied: ZnO/Al_2O_3 (50 wt% ZnO), Cu/Al_2O_3 (85 wt% CuO), Cu/ZnO (50 wt% CuO), and a $Cu/ZnO/Al_2O_3$ catalyst of industrial interest with an approximate overall composition of 50 wt% CuO, 35 wt% ZnO, and 15 wt% Al_2O_3.

The kinetic experiments were performed in a laboratory flow setup described in [21,34] which allows various temperature- and concentration-programmed experiments for the evaluation of the various catalysts to be completed in an automated way. The reactor was a glass-lined U tube (i.d. 4 mm) which could be operated up to 60 atm; 200 mg catalyst of the sieve fraction of 250–355 µm was placed between two quartz wool plugs. This particle size was found to be suitable to prevent any diffusion limitations. The following gases of highest purity were used: He (99.9999%), H_2 (99.9999%), a diluted H_2/He mixture (2.1% H_2; 99.9995%), CO/He (10% CO; 99.9995%), H_2/D_2/Ar mixture (2% H_2 (99.9999%), 2% D_2 (99.7%) in Ar (99.999%)), and a synthesis feed gas containing 72% H_2, 10% CO, and 4% CO_2, and 14% He for measuring methanol synthesis activity. Gas analysis was performed by a calibrated quadrupole mass spectrometer (Balzers GAM 422). Reduction of the catalysts was carried out in H_2/He, ramping the temperature from room temperature to 513 K. Methanol activity was measured at atmospheric pressure and at 493 K to follow catalyst deactivation during time on stream.

As shown in Fig. 1, the general procedure for carrying out the temperature-programmed experiments consisted of the following steps: subsequent to the kinetic measurements the catalyst was flushed in H_2 for 30 min at 493 K followed by flushing in He for 1 h to achieve an adsorbate-free Cu surface as a well-defined starting point for the transient experiments. In the H_2 TPD studies, the catalyst was cooled

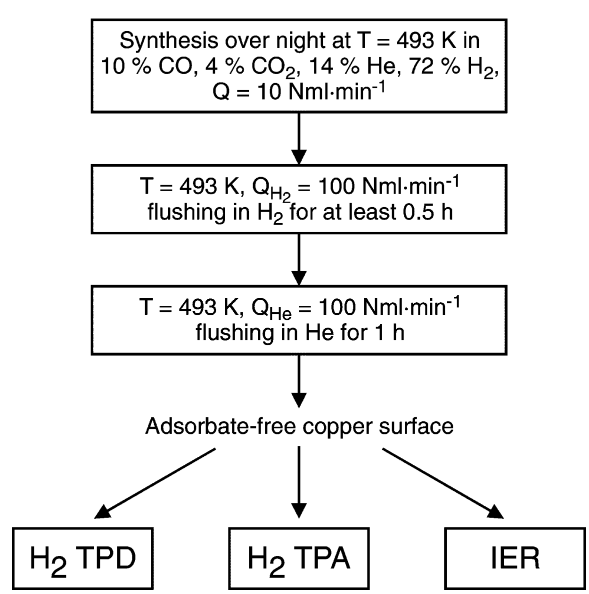

Fig. 1. General procedure for carrying out the experiments.

to 240 K in He. Previous studies in our group showed that saturation with adsorbed atomic hydrogen (H-∗) was achieved only by "high-pressure" dosing of H_2 [21], i.e., in a flow of pure H_2 for 0.5 h at 1.5 MPa and at a temperature of 240 K, which was found to be below the onset of desorption. After releasing the dosing pressure to atmospheric pressure, the reactor temperature was decreased to 78 K, and the gas flow was changed to the carrier gas He to flush the catalyst for a further 0.5 h. Then, the H_2 TPD experiment was started by ramping the temperature to 493 K ($Q_{He} = 100$ Nml min^{-1}) at heating rates ranging from 1 to 20 K min^{-1}. The upper temperature was found to be optimal to avoid sintering of the catalyst. H_2 TPA on an adsorbate-free reduced catalyst was carried out as follows: He was replaced by the diluted mixture of H_2/He at 78 K. Then, the temperature was raised at various heating rates to 493 K. Finally, the IER of H_2 with D_2 was conducted by switching under steady state conditions at 493 K from He to the mixture of H_2/D_2/Ar. IER data were acquired in a temperature-programmed way under atmospheric pressure by cooling (e.g., $\beta = -2$ K min^{-1}) followed by heating with the same rate ($\beta = 2$ K min^{-1}) to 493 K. Additional kinetic data were collected at selected temperatures under steady state reaction conditions.

3. Results

3.1. ZnO/Al_2O_3

The general pretreatment for a H_2 TPD experiment was applied to a Cu-free coprecipitated ZnO/Al_2O_3 sample subsequent to the reduction at 513 K and the carrying out of methanol synthesis at 493 K. The TPD experiment was started by switching to the carrier gas He at 78 K followed by ramping the temperature at 6 K min^{-1} to 723 K to monitor the further high-temperature desorption above 493 K. As shown in Fig. 2, no desorption peak of H_2 was observed in the relevant temperature range around 300 K and at higher temperatures. Due to the low pretreatment conditions, 0.5 mmol g_{cat}^{-1} H_2O and 0.09 mmol g_{cat}^{-1} CO_2 were detected at temperatures higher than the previously chosen reaction temperature of 493 K.

3.2. Cu/Al_2O_3

It was possible to study the dissociative adsorption kinetics on a reduced adsorbate-free catalyst in a temperature-programmed way using a dilute mixture of H_2 in He. The TPA traces obtained with the binary Cu/Al_2O_3 catalyst by using various heating rates can be seen in Fig. 3. At the beginning of the heating, residual H_2 is detected. Since the signals changed in height and position as a function of the heating rate it seems likely that they originate from the desorption of weakly bound hydrogen. A pronounced adsorption of H_2 started at 200 K independent of the heating

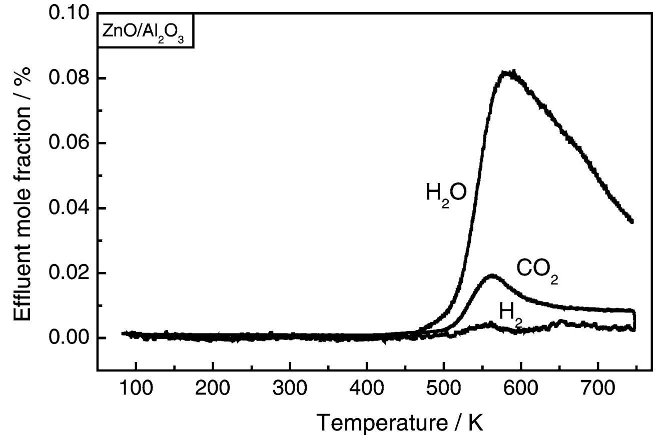

Fig. 2. H_2 TPD spectrum of a ZnO/Al_2O_3 catalyst obtained after dosing pure H_2 at 1.5 MPa and 240 K for 0.5 h. Experimental conditions: $Q_{He} = 100$ Nml min^{-1}, $\beta = 6$ K min^{-1}, $w_{cat} = 0.2$ g.

rate. This adsorption temperature indicates that the adsorption of H_2 on the Cu surface is a strongly activated process. In addition to the peak minimum temperature T_{min}, the values for the temperature T_{equal}, which specify the temperature at which the rate of adsorption and desorption are equal, are listed in Table 1. The asymmetric adsorption profile was directly followed by an asymmetric desorption profile. An increase of the heating rate resulted in a significant shift of T_{min} toward higher temperatures. The total uptake of H_2 was obtained by integrating the TPA traces from the beginning of the adsorption temperature to T_{equal}, yielding about 30% of a monolayer. Since the adsorption process is overlapped by simultaneous desorption a simple evaluation method for the determination of the kinetic parameters, i.e., the activation energy of adsorption E_{ads} and the corresponding preexponential factor, A_{ads}, is not straightforward, but will be presented in Section 3.6.

A reduced and hydrogen-covered Cu/Al_2O_3 catalyst was heated in He to 723 K. In addition to the low-temperature

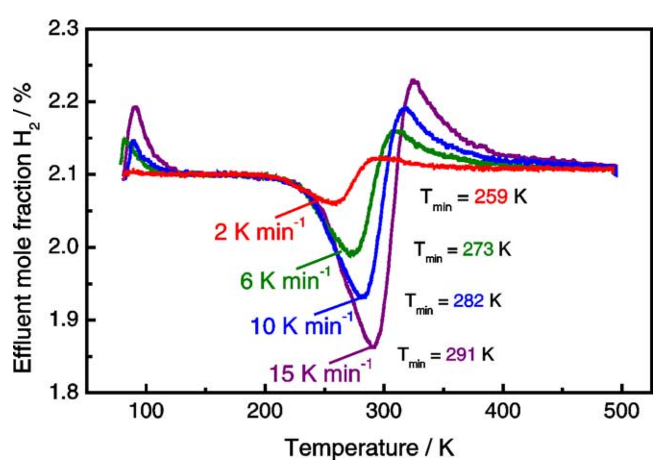

Fig. 3. H_2 TPA spectra for Cu/Al_2O_3 obtained by heating the catalyst in 2.1% H_2/He with various heating rates. Experimental conditions: $Q_{H_2/He} = 20$ Nml min^{-1}, $w_{cat} = 0.2$ g.

Table 1
T_{min} and T_{equal} obtained from H_2 TPA experiments specify the peak minimum temperature and the temperature at which the rate of adsorption and desorption are equal

Catalyst	Heating rate ($K\,min^{-1}$)	Fig.	T_{min} (K)	T_{equal} (K)	Uptake ($\mu mol\,H_2\,g_{cat}^{-1}$)	Θ_H
Cu/Al_2O_3	2	3	259	278	37	0.33
Cu/Al_2O_3	6	3	273	294	35	0.31
Cu/Al_2O_3	10	3	282	302	33	0.29
Cu/Al_2O_3	15	3	291	311	30	0.27
Cu/ZnO	6	7	285	304	38	0.37
Cu/ZnO	15	7	301	321	30	0.29
$Cu/ZnO/Al_2O_3$	2	10	270	289	50	0.50
$Cu/ZnO/Al_2O_3$	6	10	283	303	44	0.44
$Cu/ZnO/Al_2O_3$	10	10	291	310	40	0.40
$Cu/ZnO/Al_2O_3$	15	10	299	318	36	0.36

signal centered at about 300 K, a small peak at 390 K and a broad and rather complex desorption signal starting at 493 K were observed (Fig. 4). The signal at 300 K can be assigned to the H_2 desorption from metallic Cu surface sites [20–22], while the weak signal at 390 K originates from traces of water in the dosing gas, as previously shown for the $Cu/ZnO/Al_2O_3$ catalyst [34]. A complex H_2 desorption profile was detected at higher temperatures ($\geqslant$ 500 K). On the one hand, H_2 desorption has been observed in single crystal experiments [14] at 590 K from the bulk of a Cu(100) crystal. On the other hand, H_2 desorption can be attributed to the dissociation of H_2O ($Cu_s + H_2O \rightarrow Cu_sO_{ads} + H_2$), which was stored on the support in the preceding experiments. This amount of water was not removed because of the maximum pretreatment temperature of 493 K.

To study the H_2 desorption kinetics from Cu/Al_2O_3, a series of H_2 TPD experiments with variation of the heating rate was performed (Fig. 5). In each experimental run, a narrow symmetric desorption signal was recorded in the investigated temperature range of 78–493 K. The desorption peak maximum temperatures were found to shift, while the onset of the desorption signals remained constant at

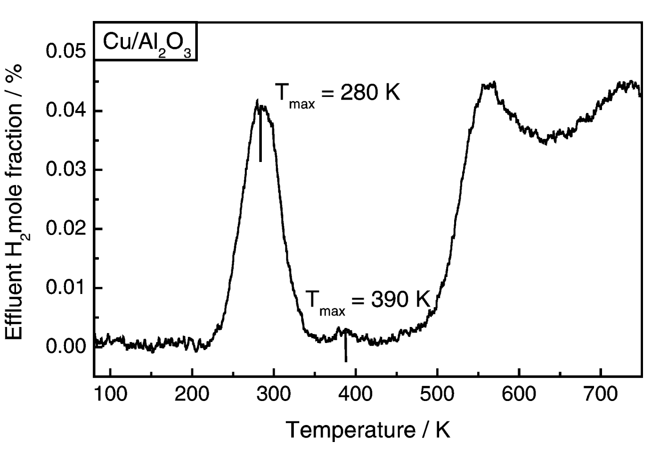

Fig. 4. H_2 TPD spectrum for Cu/Al_2O_3 obtained after dosing pure H_2 at 1.5 MPa and 240 K for 0.5 h. Experimental conditions: $Q_{He} = 100\ Nml\,min^{-1}$, $\beta = 6\ K\,min^{-1}$, $w_{cat} = 0.2$ g.

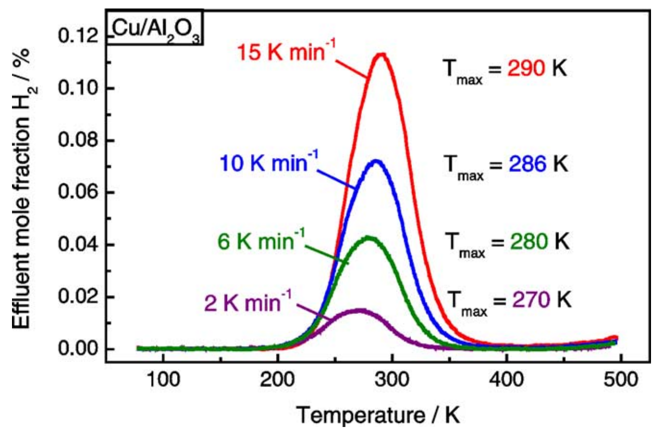

Fig. 5. H_2 TPD spectra for Cu/Al_2O_3 obtained after dosing pure H_2 at 1.5 MPa and 240 K for 0.5 h using different heating rates. Experimental conditions: $Q_{He} = 100\ Nml\,min^{-1}$, $w_{cat} = 0.2$ g.

a temperature of about 200 K. Furthermore, the relatively small full width at half maximum (FWHM) of about 60 K is remarkable for TPD experiments. All these observations are consistent with the desorption being second order. Since a strong interaction of the gas phase molecules with the catalyst can be excluded from the previously shown adsorption results, readsorption is essentially negligible. In general, readsorption leads to substantially broadened TPD peaks which are shifted toward higher desorption temperatures in a TPD run. Integration of each signal yielded about 100 $\mu mol\,H_2\,g_{cat}^{-1}$, which corresponds to a specific metallic Cu area of about 16 $m^2\,g_{cat}^{-1}$ based on a stoichiometry of Cu:H = 2:1, which was achieved as saturation coverage on Cu(111), Cu(110), and Cu(100) [10].

Fig. 6 displays the effluent H_2, D_2, and HD mole fractions as a function of the reaction temperature in the H_2/D_2 IER for the Cu/Al_2O_3 catalyst. Below a temperature of about 210 K, no exchange activity was observed. At tem-

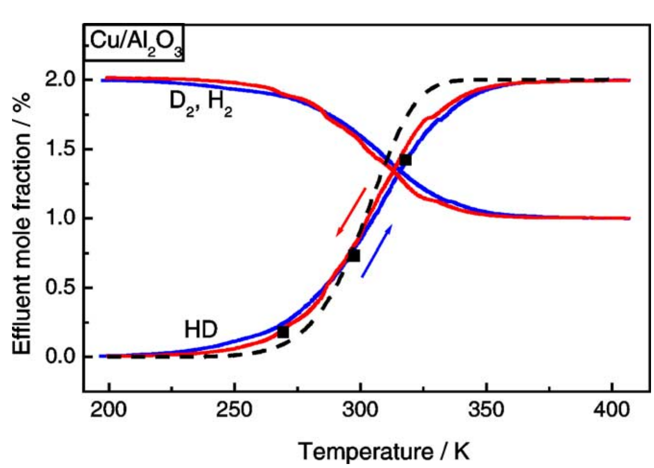

Fig. 6. H_2/D_2 IER for Cu/Al_2O_3 using a mixture of H_2/D_2 in Ar. Experimental conditions: $Q_{H_2/D_2/He} = 20\ Nml\,min^{-1}$, $w_{cat} = 0.2$ g, $\beta = 2\ K\,min^{-1}$ (ramping up), $\beta = -2\ K\,min^{-1}$ (ramping down), and at constant temperatures (squares). Dashed lines represent the simulated results using the kinetic parameters listed in Table 3.

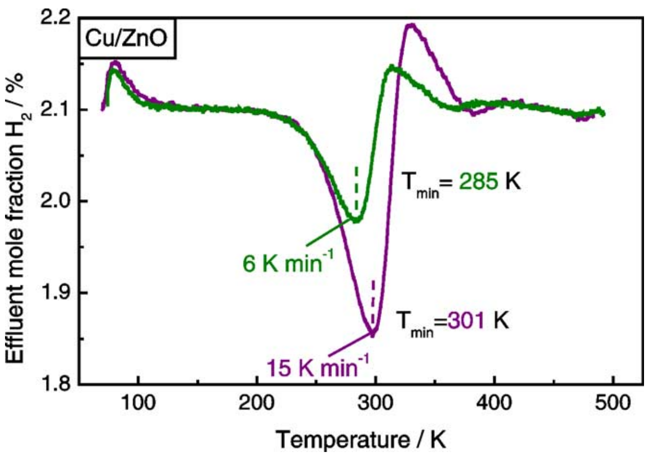

Fig. 7. H_2 TPA spectra for Cu/ZnO obtained by heating the catalyst in H_2/He. Experimental conditions: $Q_{H_2/He} = 20$ Nml min^{-1}, $w_{cat} = 0.2$ g.

peratures above approximately 370 K, the interaction becomes so fast that complete exchange is obtained under the reaction conditions applied. Ramping the temperature up (solid lines) and down (dashed lines) yielded almost identical values for the effluent mole fractions of H_2, D_2, and HD. Additionally, the exchange of H_2/D_2 was measured at selected temperatures under steady state conditions (squares). These data points agree well with the values obtained in the temperature-programmed way.

3.3. Cu/ZnO

The results for the corresponding experiments with the binary Cu/ZnO catalyst are displayed in Figs. 7–9. A closer inspection of the H_2 TPA traces (Fig. 7) revealed that the adsorption minimum temperatures and T_{equal} are somewhat higher than those obtained with Cu/Al_2O_3 (cf. Table 1). The prominent feature in the H_2 TPD experiments (Fig. 8) is the existence of the narrow symmetric peaks which are slightly shifted toward higher desorption temperatures compared

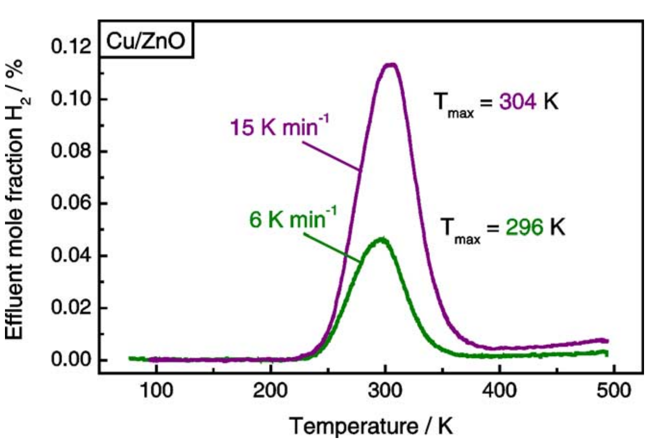

Fig. 8. H_2 TPD spectra for Cu/ZnO obtained after dosing pure H_2 at 1.5 MPa and 240 K for 0.5 h using different heating rates. Experimental conditions: $Q_{He} = 100$ Nml min^{-1}, $w_{cat} = 0.2$ g.

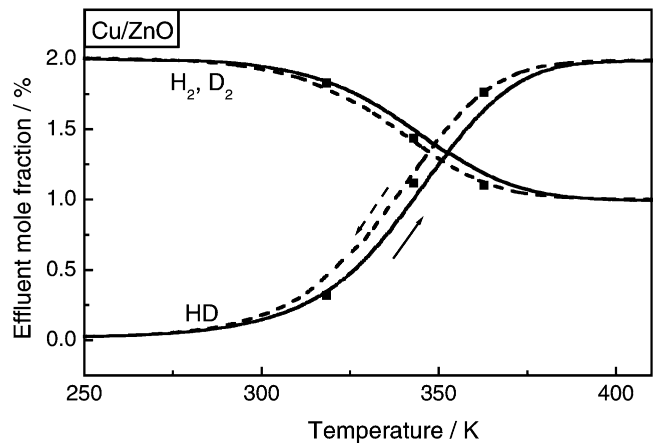

Fig. 9. H_2/D_2 IER for Cu/ZnO using a mixture of H_2/D_2 in Ar. Experimental conditions: $Q_{H_2/D_2/He} = 20$ Nml min^{-1}, $w_{cat} = 0.2$ g, $\beta = 2$ K min^{-1} (solid lines), $\beta = -2$ K min^{-1} (dashed lines), and at constant temperatures (squares).

with Cu/Al_2O_3. A mean value of about 60 K for the FWHM was measured, which agrees quite well with Cu/Al_2O_3.

A striking difference compared to the Cu/Al_2O_3 catalyst can be seen in the IER results (Fig. 9). On the one hand, the exchange reaction started at a temperature which is about 40 K higher, on the other hand, the complete exchange was achieved at substantially higher temperatures. In contrast to Cu/Al_2O_3, the traces obtained by ramping the temperature either up (solid lines) or down (dashed lines) did not coincide, indicating a pronounced hysteresis in the temperature interval ranging from 300 to 360 K. Furthermore, the data points observed under steady state reaction conditions (squares) deviate significantly from the values observed in the temperature-programmed way. The data points lie in the temperature range 340–370 K between the traces resulted from heating and cooling. At lower temperatures the steady state measurements are approximated by heating, and at higher temperatures by cooling.

3.4. $Cu/ZnO/Al_2O_3$

Finally, the same series of experiments was performed with a ternary $Cu/ZnO/Al_2O_3$ catalyst. Comparing the results for the H_2 TPA (Fig. 10) and the H_2 TPD (Fig. 11) with the traces obtained with Cu/ZnO revealed that the most pronounced features, i.e., the shape and the position of the signals, are closely reproduced. A more detailed comparison of the H_2 TPD spectra shows that the TPD signals obtained with the $Cu/ZnO/Al_2O_3$ catalyst are slightly asymmetric. The small deviations in the height of the TPD signals and in the IER traces (Fig. 12) are due to the slight difference in the specific surface areas of both catalysts.

3.5. H_2 TPD subsequent to pretreatment of CO

Instead of the general pretreatment of the catalyst with H_2 followed by flushing in He at 493 K, the Cu/Al_2O_3

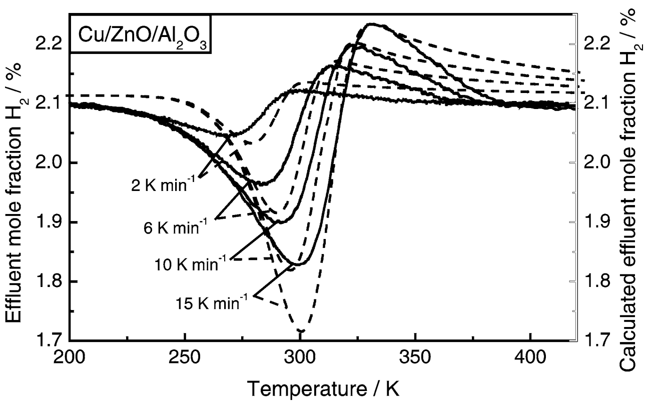

Fig. 10. H_2 TPA spectra for $Cu/ZnO/Al_2O_3$ with different temperature rates obtained by heating the catalyst in H_2/He with various heating rates. Experimental conditions: $Q_{H_2/He} = 20$ Nml min^{-1}, $w_{cat} = 0.2$ g. Simulated curves are shown as dashed lines using the kinetic Arrhenius parameters given in Table 2.

and $Cu/ZnO/Al_2O_3$ catalysts were exposed to a gas flow of 10% CO in He at 493 K for 64 h. Then, the general procedure was applied as illustrated in Fig. 1. In the case of $Cu/ZnO/Al_2O_3$, the prolonged CO/He pretreatment up to 64 h (trace B compared to trace A in the upper part of Fig. 13) led to a significant decrease in the amount of desorbed H_2 and to a reduction in the height of the main signal at 300 K. Furthermore, a second maximum in the broad signal can be identified. Alternating pretreatments of the catalyst with either CO or synthesis gas followed by flushing in He demonstrated the reversibility of the experimental findings [35]. In the case of Cu/Al_2O_3, the pretreatment with CO/He had a significant impact on the desorption profile compared to the general pretreatment (trace D compared to trace C in the lower part of Fig. 13). The onset of desorption was found to shift to much lower temperatures, while the high-temperature tailing remained. In contrast to $Cu/ZnO/Al_2O_3$, the measured amounts of desorbed H_2 were essentially equal in both experiments.

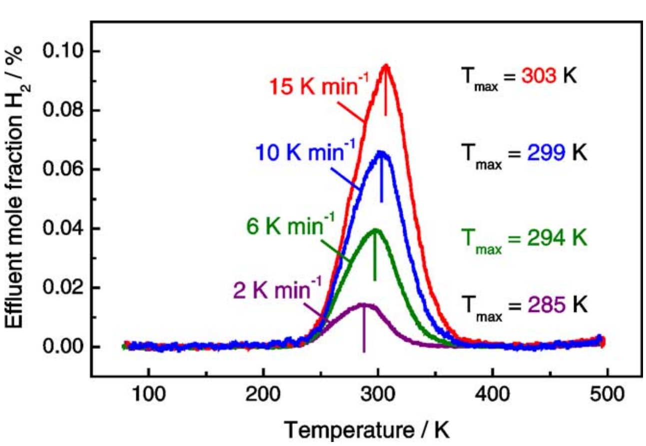

Fig. 11. H_2 TPD spectra for $Cu/ZnO/Al_2O_3$ obtained after dosing pure H_2 at 1.5 MPa and 240 K for 0.5 h with various heating rates. Experimental conditions: $Q_{He} = 100$ Nml min^{-1}, $w_{cat} = 0.2$ g.

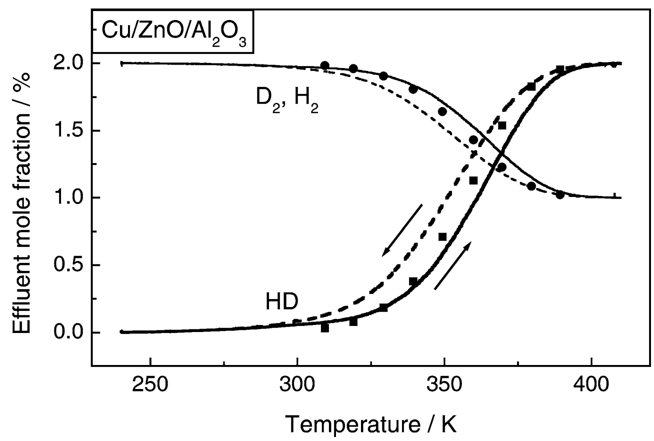

Fig. 12. H_2/D_2 IER using a mixture of H_2/D_2 in Ar. Experimental conditions: $Q_{H_2/D_2/He} = 35$ Nml min^{-1}, $w_{cat} = 0.2$ g, $\beta = 0.5$ K min^{-1} (solid lines), $\beta = -0.5$ K min^{-1} (dashed lines), and at different constant temperatures (circles, squares).

3.6. Modeling

A simple Langmuirian model with coverage-independent kinetic Arrhenius parameters was used to describe the microkinetics of the interaction of H_2 with the three Cu-based catalysts. Simulation details are given in [32]. Table 2 summarizes the kinetic parameters for H_2 adsorption. The determination is based on the following evaluation method: at T_{equal} the condition

$$2k_{ads}p_{H_2,0}(1-\Theta_H)^2 = 2k_{des}\Theta_H^2 \tag{1}$$

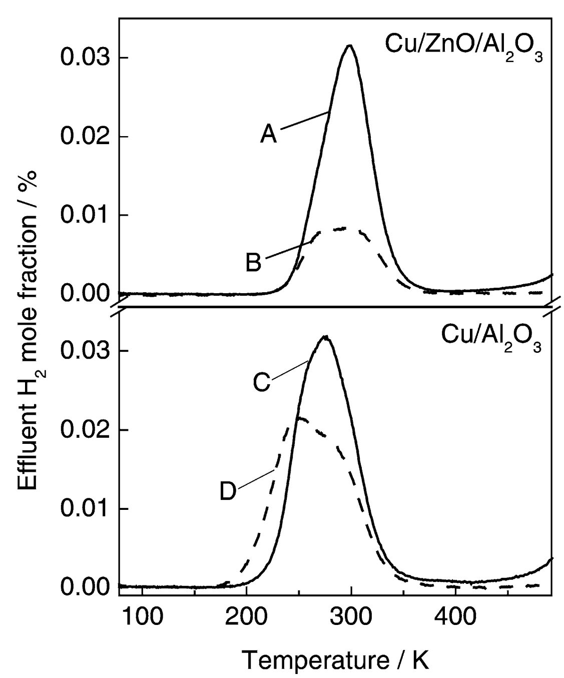

Fig. 13. Comparison of H_2 TPD spectra after general pretreatment (solid lines) and CO/He for 64 h (dashed lines). Experimental conditions: $\beta = 6$ K min^{-1}, $Q_{He} = 100$ Nml min^{-1}, $w_{cat} = 0.2$ g.

Table 2
Evaluation of kinetic parameters for the adsorption of H_2

Catalyst	Adsorption enthalpy ΔH_{ads} ($kJ\,mol^{-1}$)	A_{des}/A_{ads} (Pa)
Cu/Al_2O_3	16	4.0×10^6
Cu/Al_2O_3	22	5.0×10^7
Cu/Al_2O_3 [a]	26	–
$Cu/ZnO/Al_2O_3$	30	5×10^8

[a] Obtained by H_2 reactive frontal chromatography [23].

holds; this can be rearranged to

$$2\ln\frac{\Theta_H}{1-\Theta_{H,T_{equal}}} = \frac{\Delta H_{ads}}{RT_{equal}} - \ln\left(\frac{A_{des}}{A_{ads}p_{H_2,0}}\right) = \frac{E_{des}-E_{ads}}{RT_{equal}} - \ln\left(\frac{A_{des}}{A_{ads}p_{H_2,0}}\right). \qquad (2)$$

Plotting $2\ln\Theta_H/(1-\Theta_{H,T_{equal}})$ versus $1/T_{equal}$ should result in a straight line for ideal Langmuirian behavior. From the slope of the plot the adsorption enthalpy is directly obtained, while the intercept yields the ratio of A_{des} to A_{ads}. Fitting the TPA data results in a value for the adsorption enthalpy of 30 ± 5 $kJ\,mol^{-1}$ in the case of $Cu/ZnO/Al_2O_3$. For Cu/Al_2O_3 a value of 16 ± 5 $kJ\,mol^{-1}$ is obtained, and, if the data point for the lowest heating rate ($2\ K\,min^{-1}$) is removed, the result is 22 ± 5 $kJ\,mol^{-1}$. This clearly indicates how sensitive the evaluation method is.

The Arrhenius desorption parameters were determined from the H_2 TPD experiments based on the heating rate variation. Plotting $\ln(T_{max}^2/\beta)$ versus $1/T_{max}$ yielded the kinetic desorption parameters, i.e., the activation energy for the H_2 desorption E_{des} and the preexponential factor A_{des}. The elementary step rate constants for the second-order desorption process are summarized in Table 3. Results for the catalysts obtained in this and a previously reported study are included. In comparison to the ZnO-containing catalysts, the shift of the desorption signal maximum toward lower temperatures for the Cu/Al_2O_3 catalyst indicates that the value for the activation energy of the H_2 desorption is somewhat smaller for this catalyst. Nevertheless, E_{des} was determined to be 58 ± 2 $kJ\,mol^{-1}$, which is about 20 $kJ\,mol^{-1}$ lower than that for the ZnO-containing catalysts. Correspondingly, a physically extremely low value of 4×10^8 s^{-1} for the preexponential factor was obtained. The kinetic Arrhenius

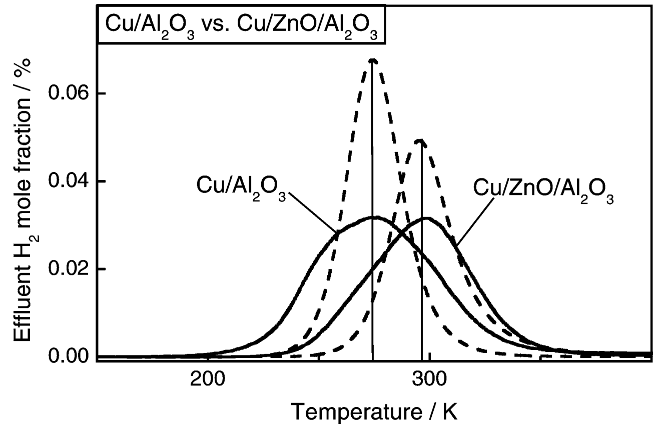

Fig. 14. Experimental H_2 TPD spectra (solid lines) and simulated curves (dashed lines) using the kinetic Arrhenius parameters given in Table 2.

parameters for the ternary catalyst, evaluated in this study, confirm those previously reported [21] exceptionally well. In the case of Cu/Al_2O_3, the same preexponential factor of 3×10^{11} s^{-1} obtained with the ZnO-containing catalysts leads to a compensated value of 72 ± 2 $kJ\,mol^{-1}$ compared to 78 ± 2 $kJ\,mol^{-1}$ for the ZnO-containing catalysts. Hence, for the modeling we assumed mean values of 50 $kJ\,mol^{-1}$ for E_{ads} and 72 and 78 $kJ\,mol^{-1}$ for E_{des} (cf. Table 2). Accordingly, the preexponential factors were approximated to obtain the best agreement between experiment and model. Simulated H_2 TPA spectra (dashed lines) are depicted additionally to the experimental spectra (solid lines) in Fig. 10. They correspond quite well in position and shape. The modeled H_2 TPD traces (dashed lines) in Fig. 14 are in good agreement with the experimental TPD traces. Since the modeled signals are narrower than the experimental signals, the underlying Langmuirian isotherm obviously underestimates the FWHM of experimental traces because of the neglected adsorbate–adsorbate and adsorbate–substrate interactions.

4. Discussion

In our TPA study of all catalysts, the striking result is that the TPA signals are not significantly altered in the presence of ZnO (Fig. 3 compared to Figs. 7 and 10). In general, the signals represent a typical adsorption profile for

Table 3
Kinetic Arrhenius parameters for the elementary rate constants for H_2 interaction $H_2 + 2* \rightleftharpoons 2H\text{-}*$

Catalyst	Dissociative adsorption		Associative desorption	
	Activation energy ($kJ\,mol^{-1}$)	Preexponential factor ($(Pa\,s)^{-1}$)	Activation energy ($kJ\,mol^{-1}$)	Preexponential factor (s^{-1})
Cu/Al_2O_3	42	1×10^2	58	4×10^8
$Cu/ZnOAl_2O_3$ (this study)	48	6×10^2	76	1×10^{11}
$Cu/ZnOAl_2O_3$ (previous study [21])	–	–	78	3×10^{11}
Parameters used for modeling				
Cu/Al_2O_3	50	2×10^3	72	3×10^{11}
$Cu/ZnO/Al_2O_3$	50	1×10^3	78	3×10^{11}

a highly activated dissociation process. The signals were found to shift with increasing heating rate toward higher temperatures. One has to bear in mind that a pretreatment in He was chosen prior to the temperature-programmed experiments to achieve an adsorbate-free reduced-Cu catalyst surface. However, additional experiments (not shown here) demonstrated that a pretreatment with CO did not significantly change the TPA profiles. In a modified manner, evaluation based on heating rate variation was done to determine the adsorption parameters, since adsorption is superimposed in the TPA spectra by desorption. We obtained the kinetic Arrhenius parameters of the dissociative adsorption of H_2 by a microkinetic analysis of a series of H_2 TPA spectra. The adsorption enthalpy was determined to be 16 $kJ\,mol^{-1}$ in the case of the Cu/Al_2O_3 catalyst, while it was found to be 30 $kJ\,mol^{-1}$ in the case of the $Cu/ZnO/Al_2O_3$ catalyst. The desorption parameters of H_2 were evaluated independently by a series of H_2 TPD experiments and were used to estimate E_{ads}. In the case of the ZnO-containing catalysts, E_{ads} of about 50 $kJ\,mol^{-1}$ was found in our measurements, which corresponds quite reasonably with the values measured on Cu single crystals.

Balooch et al. [3] measured the H_2 adsorption kinetics on Cu single crystals using pulsed supersonic molecular beams. On Cu(110) and Cu(100) they determined the activation barriers to dissociative hydrogen to be 12 and 20 $kJ\,mol^{-1}$, respectively. However, subsequent studies by different research groups determined that these values were too low [8–10,12,14]. A direct dissociation mechanism was proposed by Campbell and Campbell [12]. They determined the activation energy for the dissociative adsorption of H_2 on Cu(110) indirectly by titrating the surface oxygen by H_2. It was shown that the measured titration reaction is equal to the rate of hydrogen adsorption for oxygen coverages as $0.4 \geqslant \Theta_O \geqslant 0.2$. An activation energy of 57 $kJ\,mol^{-1}$, in close agreement with the molecular beam results of Hayden and Lamont [8,9], was obtained. Rasmussen et al. [14] measured the dissociative sticking coefficient of H_2 and D_2 on Cu(100) determined in the temperature range 215–258 K and yielding activation energies of 48 ± 6 and 56 ± 8 $kJ\,mol^{-1}$ for H_2 and D_2, respectively, which are in reasonable agreement with those obtained on Cu(110) [12].

Recently, Tabatabaei et al. [23] studied the adsorption kinetics on Cu/Al_2O_3 by reactive frontal chromatography, which was used in a manner identical to that of N_2O RFC [36]. By analysis of their hydrogen frontal line shapes they determined the activation energy to adsorption to be 42 $kJ\,mol^{-1}$ in the temperature range 213–273 K, which agrees quite well with the values measured in [37] for a Cu/SiO_2 system and with those reported in the present study.

In our H_2 TPD experiments subsequent to the general pretreatment, a single symmetric signal was observed for the Cu-based catalysts, in agreement to those of similar studies performed by various research groups [20–22]. This peak can be unequivocally assigned to second-order associative desorption from the exposed metallic Cu surface sites. The narrow widths of the signals indicate that readsorption within the catalyst bed is negligible, since this would lead to a broadening of the signals. It is important to note that complete coverage with adsorbed hydrogen was achieved only after half an hour dosing of H_2 at 1.5 MPa and 240 K followed by cooling in H_2 [21], since the evaluation of the kinetic Arrhenius parameters strongly depends on the degree of initial hydrogen coverage. The striking result of our study is that there exists only one symmetric H_2 desorption signal in the temperature range 78–493 K, which is located at 285 K in the case of the binary Cu/Al_2O_3 catalyst and is slightly shifted by 15 K toward higher temperatures in the case of the ZnO-containing catalysts. One has to bear in mind that high-pressure H_2 dosing was applied in all experiments as pretreatment, while in other kinetic studies different procedures were applied [20,22,38,39]. In our study, a second peak with substantially lower intensity at around 410 K was identified when a dosing gas contaminated with traces of water was applied during high-pressure H_2 dosing prior to the TPD experiments. Additional experiments on a partially oxidized Cu surface [34] clearly demonstrated that the second H_2 desorption peak is caused by the dissociation of H_2O released from the support.

The desorption kinetics of hydrogen from a Cu/Al_2O_3 catalyst (50:50) was also studied by Tabatabaei et al. [22] by the TPD method. In contrast to our pretreatment, the reduced catalyst was cooled in a gas flow of diluted H_2 (5% H_2 in He) from 513 to 78 K in a first series of TPD experiments. Then, the catalyst was heated in He at 5 $K\,min^{-1}$ to 600 K. A TPD spectrum with two H_2 desorption maxima located at 310 K and with a significantly lower intensity at 530 K were observed. In particular, the low-temperature peak was assigned to the H_2 desorption from exposed metallic Cu surfaces, while the high-temperature peak was assumed to originate from hydrogen which evolved from subsurface layers of the Cu metal stored during the prolonged reduction at 513 K. In a second series of TPD experiments, Tabatabaei et al. [22] derived the kinetic Arrhenius parameters from experiments performed with the Cu/Al_2O_3 as follows: different initial coverages were produced by exposing the reduced catalyst to a flow of 5% H_2 in He at atmospheric pressure and 273 K for different dosing times. Then, the catalyst was cooled in this gas mixture to 173 K followed by switching to the carrier gas He and ramping the temperature at 5 $K\,min^{-1}$ to 600 K. The TPD peak maximum temperatures were found to shift to lower values with increasing hydrogen coverages as anticipated from ideal associative second-order desorption. The resulting TPD peak for a coverage close to saturation was centered at 280 K, which is around 30 K lower than that observed in the first series of their experiment, but in an exceptionally good agreement with our TPD results, indicating that in both cases similar dosing procedures and pretreatment conditions were applied and saturation coverage of atomic adsorbed hydrogen was achieved. The line-shape analysis of the TPD signals based on the Polanyi–Wigner equation resulted in values of E_{des} decreasing from 68 to 64 kJ mol^{-1} for the activation energy of the desorption as a function of the initial coverage [22]. These parameters are in good agreement with our results. In summary it can be said that H_2 TPD results strongly depend on the chosen pretreatment conditions, in particular, on the pretreatment and dosing conditions.

The H_2 desorption kinetics from the three low-index Cu surfaces, namely Cu(111), Cu(110), and Cu(100), under UHV conditions has been studied in detail by Anger et al. [10]. From the thermal desorption spectroscopy (TDS) results, kinetic Arrhenius parameters were derived based on the Polanyi–Wigner equation. For all three surfaces a single desorption signal was obtained in the temperature range 200–400 K, which in the cases of Cu(111) and Cu(100) follows ideal second-order desorption kinetics, i.e. it varies with initial hydrogen coverage. In contrast to Cu(111), the desorption spectra of the other two Cu surfaces are more complex, deviating clearly from the expected ideal Langmuirian behavior. On Cu(100), the onset of the H_2 desorption signal was found to shift to 190 K, thus 60 K below the temperature of the desorption signal from Cu(111). Furthermore, the spectra overlapped in the high-temperature region with decreasing initial hydrogen coverage. On Cu(110), the TPD signals were found to remain at the same temperatures, just scaling in height with increasing initial hydrogen coverage. An additional low-temperature satellite peak was observed at extremely high coverages. The observed phenomena on both planes point to the fact that adsorbed atomic hydrogen induces surface reconstruction, which makes a simple analysis of the signals impossible. On Cu(110), the activation energy was found to be strongly coverage dependent, rising from 50 to 100 kJ mol^{-1} [40]. The value of 50 kJ mol^{-1} is consistent with earlier results of Wachs and Madix [41] for the desorption of D_2 from Cu(110). On Cu(111), an evaluation of the kinetic parameters is straightforward, resulting for low coverages in a value of about 77 kJ mol^{-1} accompanied with a value of 10^{-4} s^{-1} cm^{-2} for the preexponential factor. Based on a coverage-dependent analysis, E_{des} decreased linearly to about 64 kJ mol^{-1}.

Microkinetic analysis of our H_2 TPD series with the Cu/ZnO and the Cu/ZnO/Al_2O_3 catalysts based on a simple variation of the heating rate yielded values of 78 kJ mol^{-1} and 3×10^{11} s^{-1} for E_{des} and A_{des}, respectively. In general, these values are in good agreement with those derived from transition state theory and confirm previously reported results from our group [21]. Moreover, these values correspond well with those determined from TPD studies with the Cu(111) surface [10]. Hence, it can be concluded that hydrogen is desorbing from copper particles which predominantly expose Cu(111) planes under the selected general pretreatment condition. However, pretreatment with CO changes the proportions of surface sites on ZnO-containing Cu/Al_2O_3 slightly, but on ZnO-free

Table 4
Catalytic data and specific Cu surface area

Catalyst	Specific Cu surface area (m^2 g$_{cat}^{-1}$)	r_{MeOH} (μmol h^{-1} g$_{cat}^{-1}$)
Cu/ZnO	14.7	191
Cu/Al_2O_3	10	100
Cu/ZnO/Al_2O_3	11.3	250

The surface area was measured by N_2O-reactive frontal chromatography [36,54]. Methanol synthesis activity was measured at 0.1 MPa and at 493 K with a modified space velocity of 500 Nml (min g$_{cat}$)$^{-1}$.

Cu/Al_2O_3 significantly toward other crystal planes, presumably Cu(100) and Cu(110).

The modeling of the desorption signals with the experimentally determined kinetic parameters resulted in TPD profiles which correspond well both in the position and in the shape with the experimentally obtained traces. The Langmuirian model using coverage-independent kinetic parameters is sufficient thereby for the description of the experimental results. The deviation at low and high degree of coverages of H-$*$ in the experimental spectra from the modeled traces can be explained by repulsive interaction among the hydrogen atoms. Hence, coverage-dependent modeling would result in a better agreement between experiment and model, which has been shown in a previous paper [32].

The following question should be addressed in relation to catalysis: is the H_2 TPD method a relevant experiment to probe the state of the catalyst? In general, there exists a linear relationship between the methanol synthesis activity and the specific copper surface area [42]. Catalytic data were obtained for the Cu-based catalysts in a standardized test [43]. The rate of methanol formation and the results of the specific Cu surface area are listed in Table 4. The experimental results clearly underline the existence of different catalyst classes. It can be seen that the ternary catalyst is by far more active than the Cu/ZnO catalyst, although the specific Cu surface area is lower. On the other hand, Cu/ZnO shows a higher catalytic activity than Cu/Al_2O_3. In a recent paper Günter et al. [44] clearly demonstrated that, even in a systematic series with varying Cu/ZnO ratio, changes in the microstructural parameters such as the strain strongly influence the catalytic activity. The turnover frequency was found to increase with an increase in the Cu microstrain. The application of the H_2 TPD method after CO pretreatment revealed significant changes in the TPD spectra for the ternary and binary catalysts. Moreover, previous steady state kinetic measurement revealed that the catalytic activity strongly depends on the pretreatment gas applied [35]: the higher the reduction potential, the more active the catalyst. Hence, the H_2 TPD method is a valuable tool to probe the state of the active catalyst, because the dynamical morphology changes seem to be highly relevant for catalysis.

The isotopic exchange of H_2 and D_2 was measured as a complementary experiment to check the kinetics of adsorption and desorption. The kinetics is governed in a wide temperature window on the one hand by the rate of the dissociative adsorption and on the other hand by the rate of the associative desorption. The onset at lower temperatures of the H_2/D_2 exchange on the Cu/Al_2O_3 catalyst is caused by the faster rates of adsorption and desorption, respectively. The H_2/D_2 IER experiments with the ZnO-containing catalyst indicated a temperature-dependent hysteresis using the temperature-programmed method of data collection. It took hours to reach steady state for intermediate temperatures (these data points are illustrated by symbols in Figs. 6, 9, and 12). A closer inspection of the curves obtained by ramping the temperature revealed that the catalyst was in a less active state when the experiment was started at low temperature (heating cycle). At high temperatures the catalyst reaches a more active state, so that a higher IER rate is obtained in the cooling cycle. These phenomena point to a dynamic behavior of the catalyst forming highly active $CuZnO_x$ species. The dynamic modifications on the catalyst surface occur over many hours in the case of the ZnO-containing catalysts. Investigations with the ZnO-free Cu/Al_2O_3 catalyst show in fact no hysteresis in the time window of the measurement. However, significant changes in the TPD experiments subsequent to CO pretreatment were identified, which point to the fact that a transient behavior can be observed also for the Cu/Al_2O_3 catalyst under severe reducing conditions.

A dynamic behavior on Cu-based systems was also observed by other research groups [35,45–51]. In particular, the Topsøe group provided experimental evidence by applying combined XRD/EXAFS [46,50,52,53] to obtain structural data of a working 5% Cu/ZnO catalyst and to observe dynamical changes of this catalyst under “ideal” reaction conditions. This model system was studied using different methanol synthesis feed gases. The EXAFS data showed reversible changes of the coordination number of the Cu atoms upon changing the oxidation potential of the synthesis gas mixture. The coordination number increased when the catalyst was exposed to a gas with a high oxidation potential. Upon changing back to a gas with a lower oxidation potential the coordination number decreased. They interpreted their results with regard to a reversible change of the metallic Cu particle form from more spherically shaped particles with a higher apparent coordination number to more disk-like particles with a lower coordination number. Based on the Wulff construction they claimed that the flat disk-like particles expose a higher degree of Cu(100) and Cu(110) planes. Recent findings using an in situ transmission electron microscope with atomic resolution underlined that the nanocrystals undergo dynamical reversible shape changes upon changes of the gaseous environment. Lee et al. [45] reported that steady state rates were reached in catalytic experiments with a $Cu/ZnO/Al_2O_3$ catalyst after 5 and 20 h on stream upon switching from CO_2/H_2 to CO/H_2, respectively. A transient behavior has also been observed by Meitzner and Iglesia [49] on Cu/SiO_2. The catalytic activity decreased gradually over hours when they were adding CO_2 to a $CO/H_2/N_2$ mixture. Similar phenomena were also observed by our group upon switching between methanol synthesis gas and pretreatment gases such as CO and CO_2 [35].

Using the experimentally determined kinetic parameters the modeled IER curves are found to be in reasonable agreement with the experimental traces as shown exemplarily for Cu/Al_2O_3 in Fig. 6. In general, a modeling of the isotopic exchange reaction based on a simple Langmuir isotherm is very sensitive to the kinetic Arrhenius parameters chosen for modeling. Moreover, for a satisfactory description of the experimentally observed hysteresis for the ZnO-containing catalysts a dynamic microkinetic model such as the one by Ovesen et al. [47] which considers the dynamic behavior of the catalyst has to be established, e.g., a temperature- and time-dependent total number of active sites and a change in the proportion of the low-index surfaces.

5. Conclusions

We applied a combination of temperature-programmed and isotopic exchange experiments to elucidate the adsorption and desorption kinetics for Cu-based catalysts in detail. Heating rate variation was chosen as an evaluation method to extract the kinetic parameters used for microkinetic modeling.

When a pretreatment in He is applied, the subsequent H_2 TPA and TPD spectra of a Cu/ZnO catalyst correspond in shape and position with the signals obtained with the ternary $Cu/ZnO/Al_2O_3$ catalyst. Furthermore, only small differences in the kinetics of the ZnO-containing Cu catalysts and Cu/Al_2O_3 were observed. The interaction of H_2 with the Cu surfaces is therefore only slightly influenced by the presence of zinc oxide, and alumina seems to act only as a structural promoter. The H_2 TPD results were further found to depend strongly on the pretreatment conditions. This might also explain the discrepancies with respect to a correlation of surface areas and activities which still exist in the literature.

The isotopic exchange reaction turned out to be an effective experiment in identifying reversible changes occurring in the Cu/ZnO and $Cu/ZnO/Al_2O_3$ systems. The observed hysteresis point to the fact that highly mobile $CuZnO_x$ are generated under reducing reaction conditions.

The dissociative adsorption on and associative desorption of hydrogen from the Cu-based catalysts were found to obey Langmuirian kinetics of the second order. The microkinetic analysis of a series of experiments with different heating rates based on Langmuir isotherms led to elementary step rate constants which are in very good agreement with those obtained with Cu(111) under UHV conditions. The symmetrical shape and the position of the signals suggest that the ZnO-containing catalysts expose mainly the Cu(111) surface when H_2 and/or He is applied as pretreatment gas prior to TPD experiments.

Acknowledgments

The authors thank Bettina Bems for supplying the catalysts studied. Fruitful discussions with and suggestions from Martin Muhler, Robert Schlögl, Torsten Ressler, Michael Schur, Marco M. Günter, and Bettina Bems are gratefully acknowledged. This research was partially supported by the Deutsche Forschungsgemeinschaft within the scope of the Collaborative Research Center (SFB 558).

References

[1] K. Christmann, Surf. Sci. Rep. 9 (1988) 1.
[2] K. Christmann, Prog. Surf. Sci. 48 (1995) 15.
[3] M. Balooch, M.J. Cardillo, D.R. Miller, R.E. Stickney, Surf. Sci. 46 (1974) 358.
[4] J. Pritchard, T. Catterick, R.K. Gupta, Surf. Sci. 53 (1975) 1.
[5] I.E. Wachs, R.J. Madix, J. Catal. 53 (1978) 208.
[6] G. Comsa, R. David, Surf. Sci. 117 (1982) 77.
[7] K.H. Rieder, W. Stocker, Phys. Rev. Lett. 57 (1986) 2548.
[8] B.E. Hayden, C.L.A. Lamont, Phys. Rev. Lett. 63 (1989) 1823.
[9] B.E. Hayden, C.L.A. Lamont, Chem. Phys. Lett. 160 (1989) 331.
[10] G. Anger, A. Winkler, K.D. Rendulic, Surf. Sci. 220 (1989) 1.
[11] B.E. Hayden, D. Lackey, J. Schott, Surf. Sci. 239 (1990) 119.
[12] J.M. Campbell, C.T. Campbell, Surf. Sci. 259 (1991) 1.
[13] J.M. Campbell, M.E. Domagala, C.T. Campbell, J. Vac. Sci. Technol. A 9 (1991) 1693.
[14] P.B. Rasmussen, P.M. Holmblad, H. Christoffersen, P.A. Taylor, I. Chorkendorff, Surf. Sci. 287/288 (1993) 79.
[15] G.R. Darling, S. Holloway, J. Chem. Phys. 101 (1994) 3268.
[16] I. Chorkendorff, P.B. Rasmussen, Surf. Sci. 248 (1991) 35.
[17] F. Besenbacher, P.T. Sprunger, L. Ruan, L. Oelsen, I. Stensgaard, E. Lægsgaard, Top. Catal. 1 (1994) 325.
[18] J.B. Hansen, in: G. Ertl, H. Knözinger, J. Weitkamp (Eds.), Handbook of Heterogeneous Catalysis, Vol. 4, Wiley–VCH, Weinheim, 1997, p. 1856.
[19] K. Kochloefl, in: G. Ertl, H. Knözinger, J. Weitkamp (Eds.), Handbook of Heterogeneous Catalysis, Vol. 4, Wiley–VCH, Weinheim, 1997, p. 1831.
[20] M. Muhler, L.P. Nielsen, E. Törnqvist, B.S. Clausen, H. Topsøe, Catal. Lett. 14 (1992) 241.
[21] T. Genger, O. Hinrichsen, M. Muhler, Catal. Lett. 59 (1999) 137.
[22] J. Tabatabaei, B.H. Sakakini, M.J. Watson, K.C. Waugh, Catal. Lett. 59 (1999) 143.
[23] J. Tabatabaei, B.H. Sakakini, M.J. Watson, K.C. Waugh, Catal. Lett. 59 (1999) 151.
[24] M.S. Spencer, Surf. Sci. 192/193 (1987) 323.
[25] M.S. Spencer, Surf. Sci. 192/193 (1987) 329.
[26] M.S. Spencer, Surf. Sci. 192/193 (1987) 336.
[27] J.C. Frost, Nature 334 (1988) 577.
[28] M.S. Spencer, Catal. Lett. 50 (1998) 37.
[29] M.S. Spencer, Top. Catal. 8 (1999) 259.
[30] J.B. Miller, H.R. Siddiqui, S.M. Gates, J.N. Russell Jr., J.T. Yates Jr., J.C. Tully, M.J. Cardillo, J. Chem. Phys. 87 (1987) 6725.
[31] A.M. de Jong, J.W. Niemantsverdriet, Surf. Sci. 233 (1990) 355.
[32] O. Hinrichsen, F. Rosowski, M. Muhler, G. Ertl, Stud. Surf. Sci. Catal. 109 (1997) 389.
[33] B. Bems, M. Schur, A. Dassenoy, H. Junkes, D. Herein, R. Schlögl, submitted to Chem.-Eur. J.
[34] O. Hinrichsen, T. Genger, M. Muhler, Stud. Surf. Sci. Catal. 130 (2000) 3825.
[35] H. Wilmer, O. Hinrichsen, Catal. Lett. 82 (2002) 117.
[36] G.C. Chinchen, C.M. Hay, H.D. Vanderwell, K.C. Waugh, J. Catal. 103 (1987) 79.
[37] M.J. Sandoval, A.T. Bell, J. Catal. 144 (1993) 227.
[38] D.L. Roberts, G.L. Griffin, Appl. Surf. Sci. 19 (1984) 298.
[39] D.L. Roberts, G.L. Griffin, J. Catal. 110 (1988) 117.
[40] M. Golze, M. Grunze, W. Hirschwald, Vacuum 31 (1981) 697.
[41] I.E. Wachs, R.J. Madix, Surf. Sci. 84 (1979) 375.
[42] G.C. Chinchen, K.C. Waugh, D.A. Whan, Appl. Catal. 25 (1986) 101.
[43] H. Bielawa, M. Kurtz, T. Genger, O. Hinrichsen, Ind. Eng. Chem. Res. 40 (2001) 2793.
[44] M.M. Günter, T. Ressler, B. Bems, C. Büscher, T. Genger, O. Hinrichsen, M. Muhler, R. Schlögl, Catal. Lett. 71 (2001) 37.
[45] J.S. Lee, K.H. Lee, S.Y. Lee, Y.G. Kim, J. Catal. 144 (1993) 414.
[46] B.S. Clausen, J. Schiøtz, L. Grabaek, C.V. Ovesen, K.W. Jacobson, J.K. Nørskov, H. Topsøe, Top. Catal. 1 (1994) 367.
[47] C.V. Ovesen, B.S. Clausen, J. Schiøtz, P. Stoltze, H. Topsøe, J.K. Nørskov, J. Catal. 168 (1997) 133.
[48] H. Topsøe, C.V. Ovesen, B.S. Clausen, N.-Y. Topsøe, P.E. Højlund Nielsen, E. Törnqvist, J.K. Nørskov, Stud. Surf. Sci. Catal. 109 (1997) 121.
[49] G. Meitzner, E. Iglesia, Catal. Today 53 (1999) 433.
[50] J.-D. Grunwaldt, A.M. Molenbroek, N.-Y. Topsøe, H. Topsøe, B.S. Clausen, J. Catal. 194 (2000) 452.
[51] P.L. Hansen, J.B. Wagner, S. Helveg, J.R. Rostrup-Nielsen, B.S. Clausen, H. Topsøe, Science 295 (2002) 2053.
[52] B.S. Clausen, G. Steffensen, B. Fabius, J. Villadsen, R. Feidenhans'l, H. Topsøe, J. Catal. 132 (1991) 524.
[53] B.S. Clausen, L. Grabaek, G. Steffensen, P.L. Hansen, H. Topsøe, Catal. Lett. 20 (1993) 23.
[54] O. Hinrichsen, T. Genger, T. Muhler, Chem. Eng. Technol. 11 (2000) 956.